INSTABILITIES AND BUBBLE FORMATION IN FLUIDISED BEDS

Yuri Dumaresq Sobral, Y.D.Sobral@damtp.cam.ac.uk
John Hinch, E.J.Hinch@damtp.cam.ac.uk
University of Cambridge, Department of Applied Mathematics and Theoretical Physics, Wilberforce Road, Cambridge, CB3 0WA, United Kingdom

Abstract: *In this work, we investigate the concentration instabilities that occur in fluidised beds. We use the equations of motion for a two-fluid flow, proposed in Anderson & Jackson (1967), and more recently used in Anderson et al. (1995). The closure relations used to model the stress tensor of the continuum phase composed by the particles were those obtained recently in Duru et al. (2002). Confining the system to a 1D geometry, the linear and nonlinear growth and the saturation of concentration waves in fluidised beds was investigated. A linear stability analysis was carried out in order to characterise the frequency, the propagation velocity and the growth rates of small disturbances. The one-dimensional governing PDEs were then recast into a nonlinear ODE in the frame moving with the velocity of the saturated waves. This equation allows one to obtain the shape, wavelength and propagation velocity of the saturated (finite amplitude) waves. In addition, a fully nonlinear transient solution of the governing equations was obtained and the results were compared with the predictions of the linear theory and of the finite amplitude waves theory. This allowed us to explore the limits of validity of the linear theory and to set up an initial framework for future studies of two-dimensional instabilities in fluidised beds and their connections to bubbles.*

Keywords: *fluidised beds, instabilities, two phase flow, waves*

1. INTRODUCTION

Consider the flow of a fluid through a set of solid particles. The particles are supported by a perforated plate and the flow is in the upwards direction. When the flow rate is small, the fluid flows through the set of particles as if it was a porous medium. If the flow rate is increased to a level at which the drag exerted on the particles by the fluid balances their weight corrected for buoyancy, then some particles become mobile and a very small expansion of the region occupied by the particles is observed. Any further increase on the flow rate would cause the particles to become fully mobile and to occupy a larger region of the reservoir. At this stage, the particles are said to be fluidised, and the system is usually referred to as a fluidised bed. The name fluidised bed is due to the fact that the particles in this condition can be stirred and poured as a fluid [Davidson & Harrison(1963), Jackson(2000), Sundaresan(2003)].

Fluidised beds are complex systems, in which a broad range of physical phenomena are observed. For instance, fluid-particle interactions similar to sedimentation processes are observed, as well as particle-particle interactions typical of granular flows, which seem to have an important role in some kinds of fluidisation. These mechanisms of interactions and their relative importance to describe the flow do not seem to be fully understood at the present moment and are the aim of many researches.

One of the most intriguing aspects of fluidisation is its unstable behaviour. In most cases of practical applications, however, it is very difficult to obtain a particulate fluidisation, in which large gradients of concentration of particles on the scale of the fluidisation reservoir are not present. In fact, large regions free of particles, usually called bubbles, are seen to propagate along the bed and are responsible for significant changes of the dynamics of the flow. This is most commonly seen in fluidisation of particles by gases. When the fluid is a liquid, bubbles are not very frequently seen; instead, one observes the propagation of very low concentration of particles. In addition to the pure scientific motivation to understand these phenomena in fluidised beds, the vast use of such devices as industrial scale chemical reactors motivated several studies by the scientific community, with several works discussing both theoretical and experimental aspects of this flow.

Following the natural evolution of the subject so far, and mostly inspired by the works of [Duru *et al.*(2002)] and [Anderson *et al.*(1995)], the present study will aim to address relevant questions on the evolution and stability of particles concentration waves and their connections with the distinctive behaviour of liquid and gas-fluidised beds, given new constitutive equations recently proposed in [Duru *et al.*(2002)].

The present work is structured as follows. In a first stage, a linear stability analysis of small amplitude waves was carried out, aiming to understand the unstable behaviour of fluidised beds and to obtain expressions for velocity of propagation and temporal and spatial growth rates such instabilities. In a second stage, a detailed study of the saturated waves was developed, in order to understand the general behaviour of these structures. Thirdly, numerical solutions of the full governing equations for a one-dimensional fluidised bed were obtained. These allow the detailed study of the saturation process and the thorough characterisation of the waves in fluidised beds. A detailed investigation of the influence of the physical parameters on the system will be performed, in order to understand the general features of these structures.

There are evidences that the distinctive behaviour of concentration waves in liquid and gas-fluidised beds might be

due to the different levels of concentration fluctuations in the flow when the destabilisation of large amplitude saturated waves happen. It is likely that in liquid-fluidised beds, the levels of such fluctuations are low, not strong enough to trigger the instabilities that will lead to the development of secondary instabilities and then to bubbles in the flow. The study of a secondary gravitational instability, which is its ultimate goal, is still under development. This will be accomplished by a numerical solution for the two-dimensional governing equations of fluidised beds. The main interest will be focused on the prediction of the concentration fluctuation levels during the destabilisation of the saturated primary waves by secondary instabilities. In this scenario, different models of particle pressure and particle viscosity must be evaluated, since the constitutive models proposed in [Duru *et al.*(2002)] may no longer be valid.

2. Formulation of the problem

The governing equations that will be used throughout this work are those derived originally in [Anderson *et al.*(1967)], and more recently used in [Anderson *et al.*(1995)], for example. We assume that both the fluid and the fluidised particles are continua, that interpenetrate and interact through a surface without surface tension. The dynamics of these two interacting continua is therefore described by the equations of conservation of mass and momentum.

Let $\mathbf{u}$ denote the averaged velocity of the fluid phase and $\mathbf{v}$ that of the particulate phase. The local concentration of particles is ϕ, ρ stands for density and μ for dynamical viscosity, the subscripts f or s indicating if the physical property refers either to the fluid or to the particulate phase, respectively.

The continuity equation for the particulate phase and for the for the fluid phase are written as

$$\frac{\partial \phi}{\partial t} + \nabla \cdot (\mathbf{v}\phi) = 0 \quad \text{and} \quad -\frac{\partial \phi}{\partial t} + \nabla \cdot [\mathbf{u}(1-\phi)] = 0, \tag{1}$$

respectively. The momentum equation for the particulate phase is written as

$$\phi \rho_s \left(\frac{\partial \mathbf{v}}{\partial t} + \mathbf{v} \cdot \nabla \mathbf{v} \right) = \nabla \cdot \mathbf{T}_s + \mathbf{f} + \phi(\rho_s - \rho_f)\mathbf{g}, \tag{2}$$

where the stress tensor of the particulate phase is represented by $\mathbf{T}_s$ and the fluid-particle interaction force is denoted by $\mathbf{f}$. A similar equation can be written for the fluid phase:

$$(1-\phi)\rho_f \left(\frac{\partial \mathbf{u}}{\partial t} + \mathbf{u} \cdot \nabla \mathbf{u} \right) = \nabla \cdot \mathbf{T}_f - \mathbf{f} + (1-\phi)\rho_f \mathbf{g}, \tag{3}$$

where now $\mathbf{T}_f$ denotes the stress tensor of the fluid phase. The particulate phase stress tensor is defined to be

$$\mathbf{T}_s = -p_s(\phi)\mathbf{I} + \mu_s(\phi) \left[\nabla \mathbf{v} + \nabla \mathbf{v}^T - \frac{2}{3}(\nabla \cdot \mathbf{v})\mathbf{I} \right], \tag{4}$$

where $p_s(\phi)$ denotes the particle pressure and $\mu_s(\phi)$ the particle viscosity, both quantities being functions of the particle concentration. For the fluid phase, one simply writes:

$$\mathbf{T}_f = -p\mathbf{I} + \mu_f \left[\nabla \mathbf{u} + \nabla \mathbf{u}^T - \frac{2}{3}(\nabla \cdot \mathbf{u})\mathbf{I} \right], \tag{5}$$

where p is the pressure and μ_f the viscosity of the fluid phase. The fluid-particle interaction force is taken to be composed of a linear drag with respect to the relative velocities of the phases, and a virtual mass drag, based on the relative accelerations of the phases, that is:

$$\mathbf{f} = \beta(\phi)(\mathbf{u} - \mathbf{v}) + \rho_f \vartheta(\phi) \left[\left(\frac{\partial \mathbf{u}}{\partial t} + \mathbf{u} \cdot \nabla \mathbf{u} \right) - \left(\frac{\partial \mathbf{v}}{\partial t} + \mathbf{v} \cdot \nabla \mathbf{v} \right) \right]. \tag{6}$$

Here, $\beta(\phi)$ is a coefficient that is determined from the Richardson & Zaki correlation ([Richardson & Zaki(1954)] and Eq.(13) below),

$$\beta(\phi) = \frac{(\rho_s - \rho_f)\mathbf{g}}{v_t} \frac{\phi}{(1-\phi)^{n-1}}, \tag{7}$$

with v_t denoting the terminal velocity of the particles and with n being an experimental parameter. The added mass coefficient for the particulate phase, despite being dependent on the concentration of particles, is assumed to be identical to that of a single sphere, so that the reduced added mass coefficient $\vartheta(\phi)$ is given by:

$$\vartheta(\phi) = \frac{1}{2} \frac{1}{1-\phi}. \tag{8}$$

2.1 Closure of the particle phase stress tensor

The constitutive equation proposed for the stress tensor of the particulate phase needs now to be closed, i.e. the particle pressure and the particle viscosity functions need to be known. This is, in fact, the most important pressing problem in the modelling of fluidised beds using the two fluid assumption.

In this work, we shall use the particle viscosity that was obtained experimentally by [Duru *et al.*(2002)]:

$$\mu_s(\phi) = 0.18 \frac{\rho_s d_s v_t}{\phi_{rlp} - \phi}, \tag{9}$$

with ϕ_{rlp} denoting a random loose packing concentration, which is not a well-defined physical quantity.

For the particle pressure, [Duru *et al.*(2002)] also propose constitutive equations. However, their data did not allow them to propose one single expression, but rather two, depending on the choice of the density scale. These equations are:

$$\frac{dp_s}{d\phi} = \frac{7}{10}\rho_f v_t^2 \quad \text{or} \quad \frac{dp_s}{d\phi} = \frac{2}{10}\rho_s v_t^2. \tag{10}$$

Nevertheless, when this model was used on nonlinear calculations of the concentration profile, it produced spurious results, either unstable numerically or in a severe disagreement with the experimental observations from which it was derived. In fact, as clearly stated in [Duru *et al.*(2002)], the important scatter of the data for the particle could be a reflection of the large experimental uncertainly in determining the particle pressure. Moreover, the results from the linear stability analysis of their model revealed that Eq.(10) do not recover the experimental values for the critical concentration for the unset of instabilities in the fluidised bed. In fact, their value is too high, suppressing all unstable modes even for very dilute configurations of the fluidised bed.

Therefore, we have opted to use, in the present work, a particle pressure model that is available in the literature. We have chosen the ad-hoc model used by [Anderson *et al.*(1995)],

$$p_s(\phi) = \sigma\phi^3 \exp\left(\frac{r\phi}{\phi_{mp} - \phi}\right), \tag{11}$$

where ϕ_{mp} is the maximum packing concentration and σ and r are constants that should be carefully chosen in order to respect the experimental data regarding the critical concentration for each set of parameters. The values used in this work were $\sigma = 0.667$ and $r = 0.3$.

3. Linear stability analysis

In this section, we investigate the stability of small amplitude waves propagating along one dimensional fluidised beds. Therefore, the one-dimensional versions of the equations of motion, Eqs.(1) and (14), are considered. It should be noted that the momentum equation for the fluid phase is not necessary if one seeks the solutions of Eqs.(1) and (2) for ϕ, v and u, where v and u are the one-dimensional representations of $\mathbf{v}$ and $\mathbf{u}$, respectively. Moreover, by adding and integrating the one-dimensional versions of Eqs.(1), we obtain the mean flow rate in the fluidised bed q,

$$q = \phi v + (1 - \phi)u. \tag{12}$$

The quantity q is related to the homogeneous concentration in the bed ϕ_o and the particle terminal velocity by the Richardson & Zaki correlation [Richardson & Zaki(1954)], that is,

$$q = v_t(1 - \phi_o)^n. \tag{13}$$

The one-dimensional version of the momentum equation for the particulate phase is written as:

$$\phi(\rho_s + \vartheta\rho_f)\left(\frac{\partial v}{\partial t} + v\frac{\partial v}{\partial x}\right) - \phi\rho_f(1 + \vartheta)\left(\frac{\partial u}{\partial t} + u\frac{\partial u}{\partial x}\right) + \frac{\partial p_s}{\partial x} = \frac{4}{3}\frac{\partial}{\partial x}\left(\mu_s\frac{\partial v}{\partial x}\right) + \beta(u - v) - \phi(\rho_s - \rho_f)\mathrm{g}. \tag{14}$$

We proceed now to linearise the equations above around the homogeneous state of fluidisation, that is $\phi = \phi_o + \phi'$, $u = q/(1 - \phi_o) + u'$ and $v = v'$, with ϕ', u' and v' being small.

We now obtain one single equation in terms of particle concentration disturbances. This is achieved by combining the perturbed equations to successively write terms in u' and v' in terms of ϕ'. The following equation for ϕ' is obtained:

$$\mathcal{A}\frac{\partial^2\phi'}{\partial t^2} + \mathcal{B}\frac{\partial^3\phi'}{\partial x^2\partial t} + \mathcal{C}\frac{\partial^2\phi'}{\partial t\partial x} + \mathcal{D}\frac{\partial^2\phi'}{\partial x^2} + \mathcal{E}\frac{\partial\phi'}{\partial x} + \mathcal{F}\frac{\partial\phi'}{\partial t} = 0. \tag{15}$$

The coefficients in Eq.(19) are given by:

$$\mathcal{A} = -(\rho_s + \rho_f\vartheta(\phi_o)) - \frac{\phi_o}{1 - \phi_o}\rho_f(1 + \vartheta(\phi_o)), \quad \mathcal{B} = \frac{4}{3}\frac{\mu_s(\phi_o)}{\phi_o}, \quad \mathcal{C} = -\frac{2\phi_o\rho_f q}{(1 - \phi_o)^2}(1 + \vartheta(\phi_o)),$$

$$\mathcal{D} = \frac{dp_s}{d\phi}\Big|_{\phi_o} - \frac{q^2\phi_o\rho_f}{(1 - \phi_o)^3}(1 + \vartheta(\phi_o)), \quad \mathcal{E} = -\frac{\beta(\phi_o)q}{(1 - \phi_o)^2} - \frac{q}{1 - \phi_o}\frac{d\beta}{d\phi}\Big|_{\phi_o} - (\rho_s - \rho_f)\mathrm{g}, \quad \mathcal{F} = -\frac{\beta(\phi_o)}{\phi_o(1 - \phi_o)}. \tag{16}$$

3.1 First approximation: no inertia and no particle pressure

Consider initially the case where there are neither inertial effects nor particle pressure effects. This case is obtained by setting to zero in Eq.(19) the coefficients associated to inertial and particle pressure mechanisms, that is, $\mathcal{A} = \mathcal{C} = \mathcal{D} = 0$.

Imposing plane wave disturbances as $\phi' \sim \exp(i(kx - \omega t))$, where k denotes the wave number and ω the frequency of the disturbances, the simplified version of Eq.(19) becomes $\mathcal{B}k^2\omega + \mathcal{E}k - \mathcal{F}\omega = 0$, from where we can deduce that the dispersion relation of the disturbances is given by:

$$\omega = \frac{-\mathcal{E}k}{\mathcal{B}k^2 - \mathcal{F}} = \frac{c_o k}{1 + \ell^2 k^2} \tag{17}$$

where c_o is the kinematic wave speed, defined as $c_o = v_t n \phi_o (1 - \phi_o)^{n-1}$, and where the viscous length scale ℓ is defined as $\ell^2 = 4\mu_s(\phi_o)v_t(1 - \phi_o)^n / 3\phi_o \mathrm{g}(\rho_s - \rho_f)$.

The velocity of disturbances can be read off from the dispersion relation given in Eq.(17):

$$c = \frac{\omega}{k} = \frac{c_o}{1 + \ell^2 k^2}. \tag{18}$$

Therefore, we conclude that the propagation of the waves in fluidised beds is mainly dominated by viscosity, drag and weight corrected for buoyancy and that, on the absence of inertial and particle pressure mechanisms, there is neither growth nor decay of the disturbances, i.e. there is only propagation of modes with velocities given by Eq.(18).

3.2 Second approximation: with inertia and particle pressure

This is the case where the full version of Eq.(19) must be considered. Similarly to the previous case, imposing plane wave disturbances as $\phi' \sim \exp(i(kx - \omega t))$, Eq.(19) becomes:

$$-\mathcal{A}i\omega^2 + \mathcal{B}ik^2\omega + \mathcal{C}k\omega - \mathcal{D}k^2 + \mathcal{E}ik - \mathcal{F}i\omega = 0. \tag{19}$$

There are now two approaches that can be followed to investigate the stability of fluidised beds against small amplitude concentration waves: a temporal approach or a spatial approach.

To proceed with a temporal analysis, we seek a solution of Eq.(19) for ω in terms of k, assuming that the wave number of the disturbances is real and the frequency may be complex. The frequency ω has both real and imaginary parts, that is $\omega = \omega_r + i\omega_i$. Here, ω_r is actual (angular) frequency of the disturbances and is related to propagation velocity of the waves, $c_r = \omega_r / k$, and ω_i is the temporal growth rate of the disturbances. It is expected that $|\omega_i| \ll \omega_r$, in which case ω_r is roughly given by Eq.(17). With these assumptions, the following approximate expression for ω_i can be obtained:

$$\omega_i = \frac{c_r k^2}{\mathcal{E}} \left(\mathcal{A}c_r^2 - \mathcal{C}c_r + \mathcal{D} \right). \tag{20}$$

Figure 1 shows the plots of the growth rates of the disturbances, for the physical parameters presented in table 1. As stated earlier, the propagation of the waves in fluidised beds are mainly dominated by viscosity, drag and weight corrected for buoyancy, with inertia and particle pressure being only small corrections. However, inertial effects are responsible for the existence of a range of modes for which $\omega_i > 0$, as it can be observed in figure 1, that is, modes that are temporally unstable. This implies that the amplification of concentration waves in fluidised beds, i.e. its unstable behaviour, is a inertia-driven phenomena, even if only small amounts of it are involved in the process. On the other hand, particle pressure effects tend to stabilise the waves, and therefore the range of unstable modes will be determined by the competition between these two effects.

It is also observed that there is a frequency of the disturbances for which the growth rate is maximum (for this particular case, at about $f = 1.47Hz$). This will probably be the disturbance that will be observed experimentally if an unforced system becomes temporally unstable.

In some cases, especially in experiments, it is more convenient to investigate the spatial growth of the concentration disturbances rather then their temporal growth. It is also possible to investigate the spatial behaviour of these instabilities in this linear theory. In this case, it is assumed that the wave number is complex, that is $k = k_r + ik_i$, and the frequency of the disturbances is real. The real part k_r is the usual wave number and k_i is the spatial growth rate of the disturbances. Figure 1 also shows the spatial growth rates obtained from this analysis and it is observed a very similar behaviour to that of the temporal analysis. Also, the range of unstable modes obtained on both analysis is exactly the same. Note now that the maximum growth rate is now obtained for a frequency of about $f = 1.6Hz$.

A whole range of information can be obtained from the linear stability analysis. Some will be presented in the following sections, as a complimentary tool to understand the behaviour of concentration waves using different techniques.

After investigating the behaviour of the small amplitude waves is understood, we shall focus on the behaviour of the large amplitude saturated waves. The saturated waves are an intermediate state between small amplitude waves and bubbles, and may be, in fact, the link between the two structures in fluidised beds. The characterisation of the evolution from small amplitude waves to saturated waves, as well as the evolution from saturated waves to bubbles, are at the heart of the present work.

Table 1. Physical parameters of the fluidised bed investigated in this work. These values were extracted from [Duru *et al.*(2002)], combination 6.

Tube diameter	$D = 1.5 \pm 0.02\ cm$
Fluid density	$\rho_f = 0.997 \pm 0.002\ g/cm^3$
Fluid viscosity	$\mu_f = 0.9 \pm 0.02\ cP$
Particles diameter	$d_s = 685 \pm 30\ \mu m$
Particles density	$\rho_s = 4.08 \pm 0.01\ g/cm^3$
Particles terminal velocity	$v_t = 16.4 \pm 0.40\ cm/s$
Maximum packing	$\phi_{mp} = 0.612 \pm 0.005$
Random loose packing	$\phi_{rlp} = 0.580 \pm 0.005$
Homogeneous concentration	$\phi_o = 0.549 \pm 0.005$
Richardson & Zaki exponent	$n = 3.25 \pm 0.04$

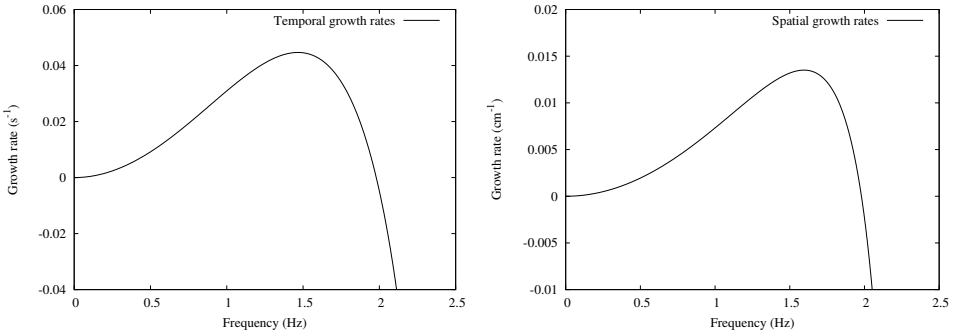

Figure 1. Growth rates of disturbances for the set of parameters in table 1. On the left, the temporal growth rate obtained from the temporal analysis and on the right the spacial growth rates.

4. Steady finite-amplitude waves regime

Experimental observations have shown that concentration waves grow along the fluidised bed and reach a saturated state: they propagate at constant velocity and their shape and amplitude do not change. Based on these observations, a simplified ordinary differential equation governing the motion of such waves was proposed in [Duru *et al.*(2002)].

Supposing that the waves propagate with constant velocity c, they are therefore stationary in the frame of reference moving with this velocity, defined by the transformation $X = x - ct$. The velocities in this frame of reference are written as $u(X) = u(x,t) - c$ and $v(X) = v(x,t) - c$, and the particle concentration is now $\phi(X) = \phi(x,t)$. The one-dimensional continuity equation for the particulate phase and the fluid phase are found to be

$$v\frac{d\phi}{dX} + \phi\frac{dv}{dX} = 0 \ \text{ and } \ -u\frac{d\phi}{dX} + (1-\phi)\frac{du}{dX} = 0. \tag{21}$$

Now, from Eq.(21), $v\phi = -c\phi_o$. Using this relation, together with Eqs.(12), (13) and (21), to eliminate u and v from the momentum equation of the particulate phase in one-dimension, the following equation in terms of particle concentration only, is obtained:

$$\frac{4}{3}c\phi_o\frac{d}{dX}\left[\frac{\mu_s(\phi)}{\phi^2}\frac{d\phi}{dX}\right] + \left[F_2(\phi) - \frac{dp_s}{d\phi}\right]\frac{d\phi}{dX} + F_1(\phi) = 0. \tag{22}$$

In this equation, $F_1(\phi)$ represents the drag and the weight corrected for buoyancy terms, and $F_2(\phi)$ represents the inertia of the fluid phase and that of the particulate phase. The expressions for these terms can be found in [Duru *et al.*(2002)]. The dynamics of the saturated waves are mostly determined by the balance between viscous effects and by the drag and weight corrected for buoyancy, the inertial and particle pressure terms being a small correction.

The major problem in finding a solution to Eq.(22) is that it is an eigenvalue problem: both the concentration profile and the velocity of propagation of the waves have to be determined by the numerical method. The process to find a solution of Eq.(22) is the following: initially, an arbitrary value of the propagation velocity is assumed in the interval $(0, c_o)$. Then, Eq.(22) is integrated by a Runge-Kutta scheme of 4^{th} order, starting from the initial state of minimum concentration and $d\phi/dX = 0$ at $X = 0$. The integration is performed until the next minimum is found, that is, after one wavelength λ is integrated. The profile that was obtained is then used to check the following integral restriction:

$$\int_0^\lambda \mu_s(\phi)\left[F_2(\phi) - \frac{dp_s}{d\phi}\right]\left(\frac{1}{\phi}\frac{d\phi}{dX}\right)^2 dX = 0, \tag{23}$$

obtained by integrating Eq.(22) over one wavelength [Duru *et al.*(2002)]. This integral is evaluated numerically by a Simpson rule. If Eq.(23) is not satisfied, then another guess for c must be tried. A bisection method is used to find c in order to satisfy Eq.(23). Therefore, the solution of Eq.(22) by this method provides not only the wave profile and the wavelength of the disturbances but also their propagation velocity.

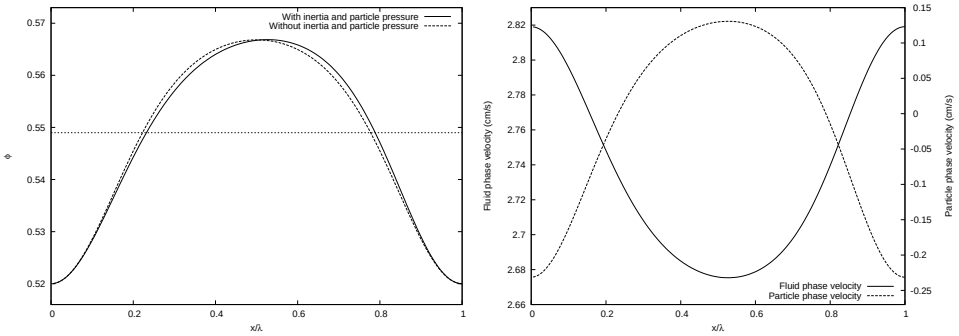

Figure 2. On the left, saturated wave profiles obtained for the configuration presented in table 1. The horizontal dashed line indicates the homogeneous value ϕ_o. On the right, velocities fields in the laboratory frame of the fluid and of the particulate phase originated by the saturated wave on the right. The propagation velocity of this wave is approximately $c = 4.1cm/s$ and its frequency is approximately $f = 1.65Hz$.

Figure 2 shows a wave profile that was integrated using the method described in the previous section. It can be observed that the concentration waves have a flat wide top, where viscous effects dominate the shape of the wave, as opposed to the inertia induced narrow regions around the minima. This is in qualitative agreement with the experiments in [Duru *et al.*(2002)]. In addition, one observes a subtle asymmetry of the wave profile, also caused by the inertia of the flow. If one neglects the inertial and particle pressure terms in Eq.(22), a symmetrical profile is obtained, as it can be seen in Fig. 2. The propagation velocity and the wavelength of the wave are almost unaffected by that simplification, as predicted by the analyses within the frame of the linearised theory.

The velocities of the phases originated by the propagation of the saturated wave in Fig.(2) on the laboratory frame can be seen in that same figure. It can be observed that the particle phase velocity is in phase with the concentration profile, whereas the fluid phase is shifted by $\pi/2$. The fluid phase velocity oscillates around the value $q/(1-\phi_o)$, that is the velocity of the fluid in the homogeneous fluidisation state. The particle phase velocity, however, oscillates around zero. This indicates that higher concentration regions travel upwards, and the lower concentration regions downwards. The latter is associated with the "rain" of particles from the lower part of a wave towards the front of the next wave, as observed in experiments.

5. Numerical solutions for the full one-dimensional problem

In order to solve Eq.(14) numerically, we had to discretise it in time and space. For space discretisation, we used a second order central differencing scheme and, for time discretisation, we used a first order Euler method, that could be either implicit (backwards Euler) or explicit (forward Euler). The time step was chosen so that both the CFL condition and, for the explicit scheme, the stability condition, were observed. In addition, the time step was such that the absolute errors associated with time-stepping were of the same order of magnitude as those observed for the spatial discretisation.

The present numerical simulations aim to reproduce the experiments that were carried out in [Duru *et al.*(2002)] and therefore the boundary conditions should reproduce the experimental setup. On the experiments, the fluidised bed was excited by a piston located on the entrance of the bed (also working as a distributor) that oscillated with controlled frequency and amplitude. This condition is reproduced numerically by setting the concentration at the entrance as $\phi_{ent} = \phi_o\left[1 + \varepsilon\sin(2\pi f t)\right]$, where f is the frequency and ε is the amplitude of the oscillations. Given the concentration, the velocity of the particulate phase at the entrance of the bed is given by the condition that the drag and weight corrected for buoyancy balance each other. This gives $v_{ent} = q - v_t(1-\phi_{ent})^p$. Finally, the fluid velocity at the entrance is then calculated using Eq.(12). Note that ε is the input amplitude of the excitation on the boundary. The saturated state does not depend on the value of ε. It is solely define by the physical parameters of the system and the frequency of excitation.

The exit condition is more complicated. In the experiments, the particles occupy only a section of the fluidised bed and at the top of the fluidised bed there were no particles, only fluid. Therefore, it would be sensible to set zero particle concentration and velocity at the exit. However, this would imply solving the Navier-Stokes equation for the clear fluid and an evolution equation for the shape and the position of the interface of the fluidised bed. This would introduce more uncertainties to the present model. In the present work, however, we have opted to detour all these difficulties and impose free exit condition for the waves on the top boundary of the fluidised bed. This choice is due to the fact that we are simulating only the region occupied by the particles on the fluidised bed, i.e., there are particles all over the integration domain. Numerically, this condition is obtained by imposing zero second derivatives at the exit, so that the waves can exit

the integration domain without affecting the solution, that is:

$$\frac{\partial^2 \phi}{\partial x^2}\Big|_{exit} = \frac{\partial^2 v}{\partial x^2}\Big|_{exit} = 0. \tag{24}$$

Finally, the initial condition for the simulations is the homogeneous fluidisation state, that is $\phi(x,0) = \phi_o$, $v(x,0) = 0$, and $u(x,0) = q/(1-\phi_o)$.

In addition to those boundary conditions, we also set up another numerical experiment that could allow the investigation of the temporal behaviour of the disturbances. This is achieved by using periodic boundary conditions on the integration domain and a small amplitude sinusoidal concentration wave of a given λ wavelength as initial condition, that is $\phi(x,0) = \phi_o\left[1 + \varepsilon \sin\left(2\pi x/\lambda\right)\right]$. The velocities of the phases were calculated accordingly to match this initial condition.

Figure 3 shows the wave profile of saturated waves obtained from the numerical integration of the full nonlinear governing equations. It can be observed the typical shape of the concentration waves in fluidised beds, that is the flat top near maximum concentrations, the thin region near minimum concentration and the asymmetry of the waves. The latter feature is due to the fact that particles fall from the lower face of a concentration wave and stop suddenly when they hit the upper face of the next wave, as discussed previously.

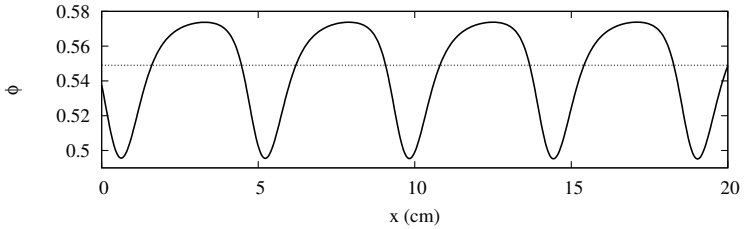

Figure 3. Wave profile in the fluidised bed. Simulation run for the parameters presented in table 1 with excitation frequency of $f = 1Hz$ and $\varepsilon = 0.04$. Time step was $\Delta t = 1.25 \cdot 10^{-4} s$ and space step was $\Delta x = 3 \cdot 10^{-2} cm$. The x-coordinate represent relative positions on the fluidised bed. The horizontal dashed line indicates the homogeneous value ϕ_o.

The code was validated by taking very small amplitude waves and tracking their growth along the fluidised bed and compare their growth rates and wavelengths with respect to those predicted by the linear stability theory. The result can be seen in Fig.(4), where a very good agreement of the numerical results with the linear theory is observed.

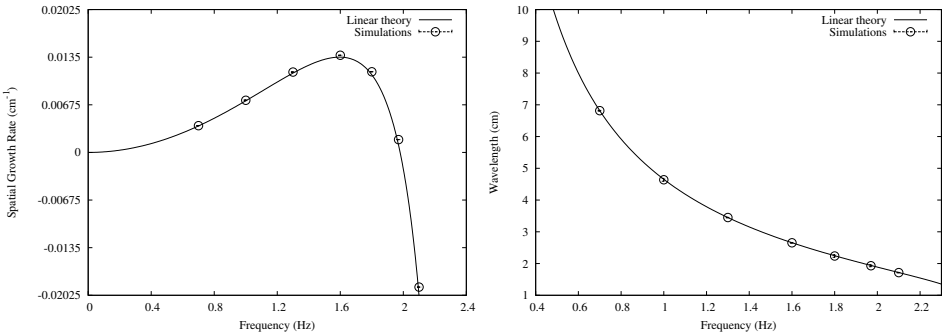

Figure 4. Validation of the code for very small amplitude waves. On the left, the growth rate of the waves and on the right, the wavelength of the waves. Results obtained for the parameters as in table 1.

6. Results and discussion

The evolution of the small amplitude waves towards saturation can be observed in Fig. 5. The linear stability theory predicts the growth of the waves correctly until up half way through saturation, at amplitudes of around 0.1. After that, a slower growth rate is observed and the waves evolve slowly until saturation is reached. It should be stressed that the saturated waves are a property of the system and are not dependent on the amplitude of excitation at the distributor.

The strong nonlinearity in this systems cause some higher harmonics disturbances to be excited and, sometimes, to propagate along the fluidised bed together with the desired excited wave. Figure 5 (right) shows the power of the waves in Fig. 5 (left). In this case, the nonlinearity is small and the major mode propagating is effectively the excited mode. This is because the mode with frequency $1.6Hz$ is the most unstable mode for this configuration and it grows quicker than any other mode in the bed and, in fact, the higher harmonics have negative growth rates and will decay quickly as they propagate. However, for very low frequencies of excitation, a strong influence of higher harmonics on the wave profiles is observed. In these cases, some of the higher harmonics have positive growth rates; they grow along the bed

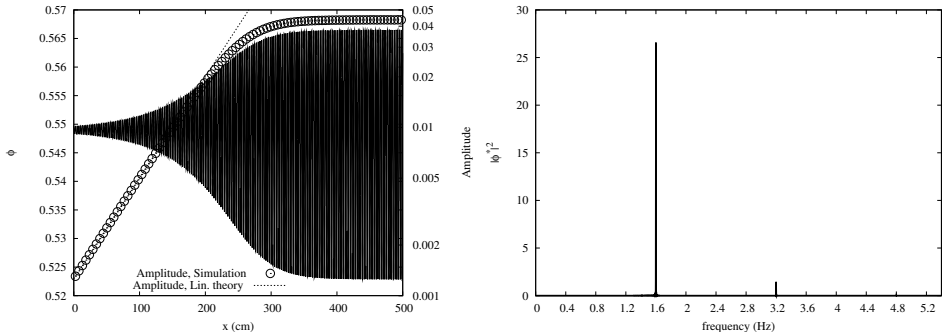

Figure 5. On the left, evolution of the disturbances towards a saturated state. The particle concentration is plotted heavy lines, and the amplitude of the waves obtained from the simulations is plotted with dots. The linear theory prediction is plotted with dashed lines. On the right, the spectrum of these waves. Results obtained for $1.6Hz$.

and interfere with the originally excited mode, leading to the formation of waves with secondary minima. This was also observed experimentally by [Duru *et al.*(2002)].

Bearing that in mind, we now start to analyse the properties of the saturated wave profiles. The shape of the saturated wave profiles change significantly with the frequency of excitation, as can be observed in Fig.6. Lower frequency modes are more asymmetric and have much larger amplitudes. In fact, this can be understood from the linear stability analysis. As observed above, the absence of inertia and particle pressure in the model created modes with no growth rates, that only propagated along the bed with velocity given by Eq.(18). Therefore, neutral modes are modes in which inertial and particle pressure mechanisms balance perfectly. The dispersion relation curves, presented in Fig. 1, show that as the frequency of the disturbances is increased from low frequencies, there will be a frequency with zero growth rate and, therefore, modes with frequencies close to that will tend to have smaller imbalances of inertia and particle pressure and will tend to have smaller amplitudes (tending towards the excitation amplitude in the limit of the neutral growth frequency). This explains why the asymmetry and amplitude of the high frequency modes is very small.

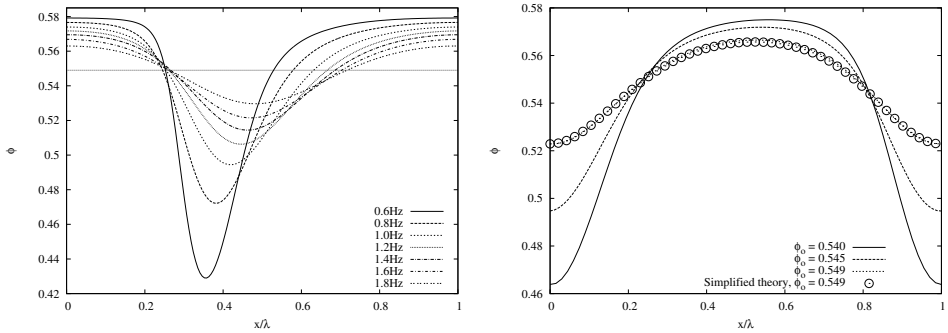

Figure 6. On the left, the influence of the frequency of excitation in the shape of the saturated waves. On the right, the influence of the homogeneous concentration in the shape of the saturated waves. The dots represent the solution obtained with the saturated wave theory. Results obtained for $1.6Hz$ and for the parameters as in table 1. The horizontal dashed line indicates the homogeneous value ϕ_o. Note the asymmetry of the thin region on lower concentrations and the wide region of large concentrations.

The influence of the homogeneous concentration can also be seen in Fig. 6. For the same excitation frequency, in more concentrated fluidised beds, the waves tend to have smaller amplitudes and less asymmetries. This can be seen from Eq.(22), where the inertial and particle pressure terms compete directly to change the shape of the wave. Higher concentration beds will have higher levels of particle pressure and the imbalance with the inertial term will be smaller. Also in Fig. 6, a comparison of the concentration profiles obtained with the simplified theory and with the full numerical solution is presented. A very good agreement is observed. The small differences might be accounted by higher harmonics propagating on the flow.

Figure 7 shows the stability diagram for the parameters presented in table 1. This diagram is obtained by collecting all the frequencies for which the growth rate is zero from the dispersion relation of the disturbances, for different values of a control parameter, in this case the homogeneous concentration. In addition, we have added the experimental points of [Duru *et al.*(2002)] for which they have observed unstable behaviour (saturated waves). We also plotted the results from our simulations and the general agreement is good. However, there are two results that do not follow the predicted behaviour from the linear theory. The first one is the experimental observation for $f = 2.2Hz$ at $\phi_o = 0.549$. Here, [Duru *et al.*(2002)] have managed to excite a wave of this frequency experimentally, whereas the linear theory predicts that this frequency should be stable. In fact, the might be a problem with the choice in the particle pressure, as it will be discussed in detail at the end of this section. The other is the simulation result for $f = 3Hz$ at $\phi_o = 0.535$; this turned

out to be an unstable point. In fact, for homogeneous concentrations of around $\phi_o = 0.537$ and lower, the simulation results are all unstable and they have the special property that the saturated state does not have the same frequency as the one excited originally. In fact, the system will always shift to the most unstable (*global*) mode and this will dominate the dynamics of the flow, it does not matter what the excitation frequency is. The homogeneous concentration $\phi_o = 0.537$ is the one for which the mode with zero group velocity has zero growth rate. For lower concentrations, the growth rates of these modes are positive and, therefore, a sort of absolute instability, as opposed to the convective instability, takes place. A more detailed discussion of this can be found in [Nicolas *et al.*(1994)] and [Nicolas *et al.*(1996)].

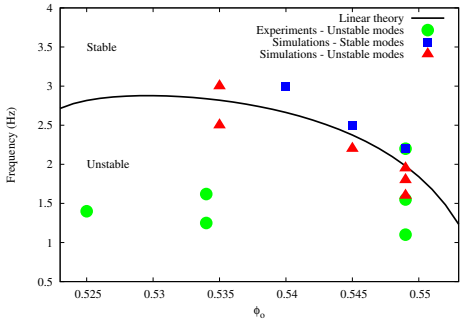

Figure 7. Stability diagram for the fluidised bed with parameters as in table 1.

We now analyse quantitatively the properties of the waves. Figure 8 shows the results obtained for the wavelengths of the waves, as predicted by all the methods used in this work. A very good agreement between the saturated waves theory and the simulations with the linear predictions is observed for higher frequency notes. The experimental points from [Duru *et al.*(2002)] also indicate that the results are consistent with the experiments. However, lower frequency modes, very nonlinear, have wavelengths that differ from the linear stability predictions. This indicates that the the wavelength is set at lower amplitudes, governed mainly by viscous effects on the particulate phase.

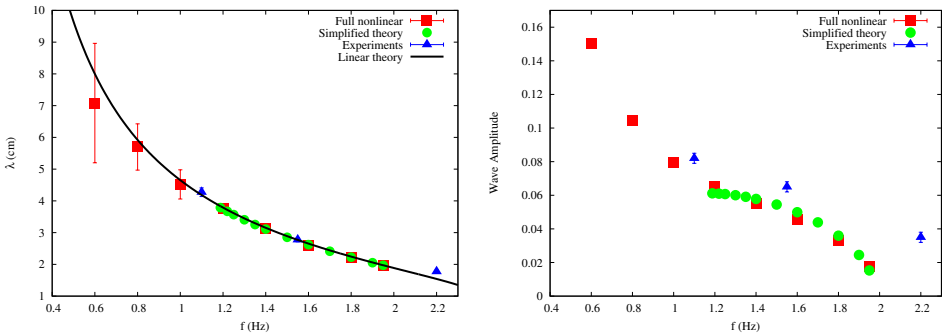

Figure 8. On the left, wavelength of the disturbances for different frequencies. On the right, amplitude of the disturbances for different frequencies. Results obtained for the parameters as in table 1.

The good quantitative agreement observed for the wavelengths of the disturbances is not observed for the amplitudes. The results plotted in Fig. 8 show that the results underestimate the amplitude of the waves by an important amount, when compared with the experimental results from [Duru *et al.*(2002)]. This will be discussed below. Also from Fig. 8, one observes that the saturated waves theory predicts a different trend from that predicted by the simulations. In fact, the simplified theory was unable to find low frequency saturated waves. This is still under investigation, but the indication is that this is somehow related to the particle pressure uncertainties.

In fact, the influence of the particle pressure on the amplitude of the waves is significant and, therefore, uncertainties on the model might be at the heart of the discrepancies found in this work. The choice of the particle pressure model was based on previous works and supported by the lack of more consistent models. The choice of the constants σ and r appearing on the model had the be careful, in order to respect the critical concentration for the onset of instabilities. However, this choice is not unique. Table 2 shows four possible combinations of parameters that will respect the experimental critical concentration for the onset of instabilities for the set of parameters in table 1.

Using the combinations of parameters presented in table 2, the dispersion relations and the saturated wave profiles could be obtained, and are shown in Fig. 9. The dispersion relations show that the behaviour of the modes is significantly altered by the changes in the particle pressure. For instance, modes of frequency $f = 1.6Hz$ can either be stable or unstable, with growth rates varying roughly 3 times. Also, the most unstable modes change, as well as the neutral modes (and, therefore, the neutral lines). Looking at the saturated wave profiles, not only the shape of the waves change, but also its amplitude. Therefore, discrepancies in Fig. 8 are related to the particle pressure choice. Unfortunately, since a reliable

and consistent model for particle pressure has not been obtained, either experimentally or theoretically, most of the results will have a strong qualitative character, but will lack in experimental quantitative comparisons.

Table 2. Particle pressure constants σ and r

Combination 1	$\sigma = 51.766$	$r = 0.03$
Combination 2	$\sigma = 0.667$	$r = 0.3$
Combination 3	$\sigma = 0.01879$	$r = 0.6$
Combination 4	$\sigma = 0.0006853$	$r = 0.9$

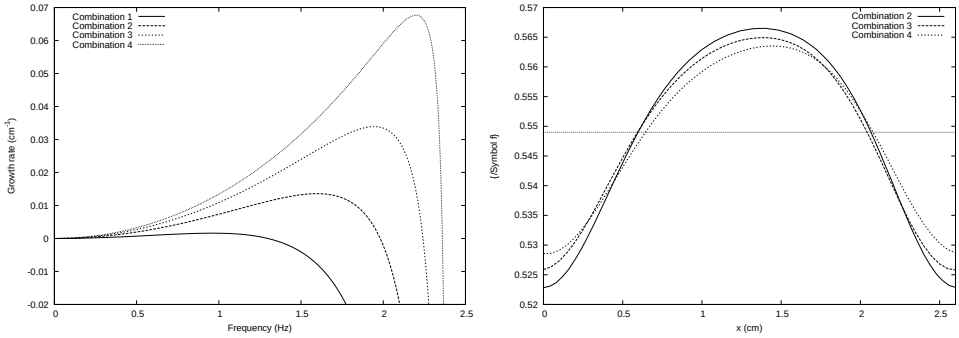

Figure 9. On the left, dispersion relations for small amplitude disturbances with physical parameters as in table 1, but with particle pressure coefficients as in table 2. On the right, the resulting saturated profiles. Combination 1 in table 2 and a frequency of $1.6Hz$ produce a stable mode. The horizontal dashed line indicates the homogeneous value ϕ_o.

7. Final remarks

In this work we have investigated the behaviour of one-dimensional instabilities in fluidised beds, from the range of very small amplitudes to finite amplitude steady states. This is the base study for a two-dimensional study that is currently in progress. We want to undertake fully nonlinear transient solution of the governing equations to investigate the secondary instability in fluidised beds. Such instabilities are transversal destabilisation of the primary (one-dimensional) instabilities and might be connected with the formation of bubbles in fluidised beds, [Batchelor(1993), Batchelor & Nitsche(1991)]; of which strong experimental evidence now exists in [Duru & Guazzelli(2002)]. Our next step is to try and establish the connection of secondary instabilities with the formation of bubbles in fluidised beds and propose criteria that could account for the different behaviour of liquid and gas-fluidised beds. Y.D. Sobral would like to thank the financial support received from the Capes Foundation - Ministry of Education of Brazil.

8. References

Anderson, K., Sundaresan, S., Jackson, R. Instabilities and the Formation of Bubbles in Fluidized Beds, Journal of Fluid Mechanics, Volume 303, 327–366 (1995)

Anderson, T. B. , Jackson, R. A Fluid Mechanical Description of Fluidized Beds: Equations of Motion. I&EC Fundamentals, Volume 6, 527 – 539 (1967)

Anderson, T. B. , Jackson, R. A Fluid Mechanical Description of Fluidized Beds: Stability of the Uniform State of Fluidization. I&EC Fundamentals Volume 7, 12 – 21 (1968)

Batchelor, G. K., Nitsche, J. M. Instability of stationary stratified fluid. Journal of Fluid Mechanics, Volume 227, 357 – 391 (1991)

Batchelor, G. K. Secondary Instability of a Gas-Fluidized bed. Journal of Fluid Mechanics, Volume 257, 359 – 371 (1993)

Davidson, J.N., Harrison, D. Fluidized Particles. Cambridge University Press, Cambridge, UK (1963)

Duru, P., Guazzelli, E. Experimental Investigation on the Secondary Instability of Liquid-Fluidized Beds and the Formation of Bubbles. Journal of Fluid Mechanics, Volume 470, 359 – 382 (2002)

Duru, P., Nicolas, M., Hinch, E.J., Guazzelli, É. Constitutive Laws in Liquid-Fluidized Beds.Journal of Fluid Mechanics, Volume 452, 371 – 404 (2002)

Jackson, R., The Dynamics of Fluidized Particles. Cambridge University Press, Cambridge, UK (2000)

Nicolas, M., Chomaz, D., Guazzelli, E. Absolute and Convective Instabilities of Fluidized Beds. Physics of Fluids, Volume 6, 3936 – 3944 (1994)

Nicolas, M., Chomaz, J.-M., Vallet, D., Guazzelli, E. Experimental Investigations on the Nature of the First Wavy Instability in Liquid-fluidized Beds. Physics of Fluids, Volume 9, 1987 – 1989 (1996)

Richardson, J. F., Zaki, W. N. Sedimentation and Fluidization. Trans. Inst. Chem. Engrs., Volume 32, 35 – 52 (1954)

Sundaresan, S., Instabilities in Fluidized Beds. Annual Review of Fluid Mechanics, Volume 35, 63 – 88 (2003)